Comparison of δ^{18}O analyses on individual planktic foraminifer (*Orbulina universa*) shells by SIMS and gas-source mass spectrometry

Jody B. Wycech[a],[*], Daniel Clay Kelly[a], Reinhard Kozdon[b], Ian J. Orland[a], Howard J. Spero[c], John W. Valley[a]

[a] Department of Geoscience, University of Wisconsin-Madison, 1215 W. Dayton St., Madison, WI 53706, USA
[b] Lamont-Doherty Earth Observatory of Columbia University, 61 Route 9W, Palisades, NY 10964, USA
[c] Department of Earth & Planetary Sciences, 1 Shields Ave, University of California Davis, Davis, CA 95616, USA

ABSTRACT

The oxygen isotope (δ^{18}O) compositions of final chamber fragments of individual shells of the planktic foraminifer *Orbulina universa* were measured *in situ* via secondary ion mass spectrometry (SIMS) and by traditional gas-source mass spectrometry (GSMS) entailing acid digestion of sampled calcite. The paired SIMS-GSMS analyses were performed on final chamber fragments of fossil shells taken from the top of a sediment core (Holocene) as well as shells grown in laboratory culture. Multiple iterations of SIMS-GSMS analyses were conducted on final chamber fragments treated with a variety of cleaning protocols. The series of paired analyses yielded an average SIMS-GSMS δ^{18}O offset ($\Delta^{18}O_{SIMS-GSMS}$) of -0.9 ± 0.1‰ ($\pm$ 2 SE). The volume of material analyzed in 10-μm SIMS spots is ~10^5 times smaller than that analyzed by GSMS; hence, the extent to which these $\Delta^{18}O_{SIMS-GSMS}$ values represent real differences in analyte vs. instrumental factors remains unclear. Possible contributing factors to the SIMS-GSMS δ^{18}O difference include sample-standard mismatch by SIMS, differences in standardization of SIMS and GSMS, and non-calcite contaminants in samples. Although the two datasets are consistently offset, SIMS values reproduce inter-shell δ^{18}O variability delineated by shell fragment GSMS values. This strong positive covariance proved useful for bringing the two datasets into agreement (i.e. $\Delta^{18}O_{SIMS-GSMS}$ = 0), and confirms that SIMS-based foraminifer δ^{18}O values record changes in calcification temperature and/or δ^{18}O of seawater. Whether shells of foraminifer taxa with differing microcrystalline structures, chemical composition, and/or preservation histories register a similar $\Delta^{18}O_{SIMS-GSMS}$ value is a subject of ongoing testing.

1. Introduction

Oxygen isotope ratios (^{18}O/^{16}O) measured from the biogenic calcite of microscopic shells grown by foraminifera, an extant group of marine protists with a rich fossil record, are one of the most widely used geochemical proxies for reconstructing past ocean-climate change (Pearson, 2012). However, reconstructions of ocean-climate history require the use of foraminifer shells that have retained their original oxygen isotope (δ^{18}O) composition over time. Unfortunately, there is a paucity of pristinely preserved material in the deep-sea sedimentary archive as the chemistries of fossil foraminifer shells are often altered through isotopic exchange with sedimentary pore fluids (e.g. Killingley, 1983; Schrag et al., 1995; Pearson et al., 2001). To complicate matters, an added source of intra-shell δ^{18}O variability stems from the complex life histories and ecologies of planktic foraminifera. Such sources of intra-shell δ^{18}O heterogeneity are problematic for paleoclimate studies using conventional gas-source mass spectrometry (GSMS) because these

analyses require acid digestion and isotope ratio measurements of whole shells that are often aggregate mixtures of carbonate that precipitated under differing environmental, ecological, and physiological conditions (e.g. Lohmann, 1995).

Over the past decade, the WiscSIMS laboratory has developed analytical techniques and procedures to address the aforementioned challenges to conventional GSMS δ^{18}O analyses. To this end, secondary ion mass spectrometry (SIMS) is now being used to make *in situ* δ^{18}O measurements on micrometer-scale domains within carbonate minerals, including individual foraminifer shells (Valley and Kita, 2009; Kozdon et al., 2009, 2011; Kita et al., 2009; Vetter et al., 2013). The ultra-high spatial resolution (~1–10 μm) of SIMS analyses permits isolated measurement of δ^{18}O in only the desired domain of an individual shell, and has been used to quantify the effects of diagenesis on the δ^{18}O of fossil planktic foraminifer shells (Kozdon et al., 2013) and delineate intra-shell δ^{18}O signals that reflect experimentally induced geochemical bands in cultured planktic foraminifers (Vetter et al., 2013). SIMS has
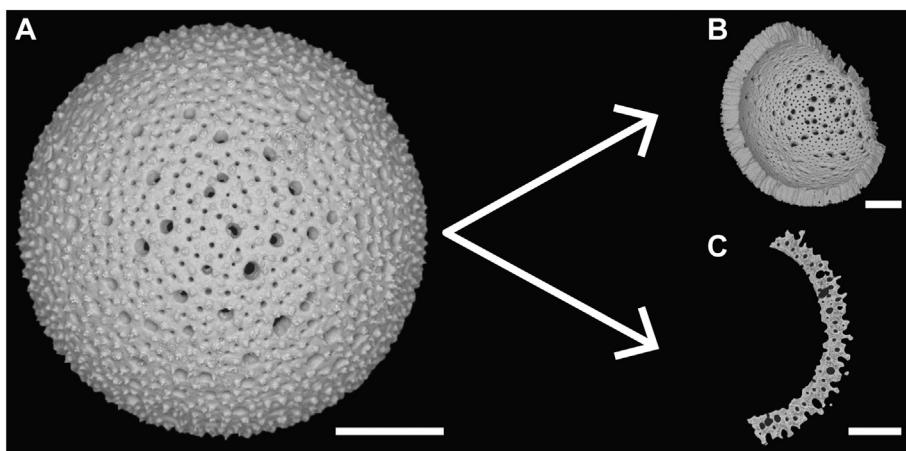
Fig. 1. Scanning electron microscope (SEM) images depicting chamber fragmentation method used in this study. All scale bars are 100 μm. A. Back-scattered electron (BSE) SEM image of intact *O. universa* shell taken from the core-top of PC9. B. BSE SEM image of the final chamber fragment used for GSMS analysis. C. Secondary electron (SE) SEM image of remaining fragment cast in epoxy and cross-sectioned for SIMS analysis.

likewise been used to interrogate micrometer-scale $\delta^{18}O$ variability in carbonate materials as varied as corals (Rollion-Bard et al., 2007; Allison et al., 2010), nautiloids (Linzmeier et al., 2016), bivalves (Vihtakari et al., 2016), otoliths (Weidel et al., 2007; Hanson et al., 2010), and speleothems (Kolodny et al., 2003; Treble et al., 2007; Orland et al., 2009; Liu et al., 2015).

The aforementioned studies indicate that the use of SIMS to perform *in situ* $\delta^{18}O$ analyses on micrometer-scale domains within low-temperature carbonates represents a fundamental advance for enhancing the fidelity of paleoclimate reconstructions. Yet the potential of this technique cannot be fully realized without comparison to traditional whole-shell $\delta^{18}O$ values measured by GSMS. A tendency has emerged for SIMS measurements of $\delta^{18}O$ in low-temperature carbonates, at WiscSIMS and other labs, to be consistently lower than "paired" GSMS $\delta^{18}O$ values (Orland et al., 2015). Differences in GSMS and SIMS $\delta^{18}O$ data of typically 0–2‰ in biocarbonates and speleothems may arise from unrecognized analytical biases in the two techniques. The cause(s) of the previously observed SIMS-GSMS $\delta^{18}O$ difference ($\Delta^{18}O_{SIMS-GSMS}$) remains unclear and identifying the mechanism is beyond the scope of this study; nevertheless, few studies have directly compared SIMS and GSMS $\delta^{18}O$ measurements on the same material (Kozdon et al., 2011; Orland, 2012; Orland et al., 2015). Here, we conduct an inter-instrument $\delta^{18}O$ comparison by analyzing planktic foraminifer calcite using the extant, mixed-layer dwelling species *Orbulina universa*.

The species *O. universa* was selected for three reasons: (1) field and culturing studies have established the ecological affinities of this symbiont-bearing, mixed-layer species (e.g. Spero and Parker, 1985; Hemleben et al., 1989), (2) the relationship between $\delta^{18}O$ and temperature in *O. universa* calcite has been empirically calibrated and shown to be very reproducible (e.g. Bemis et al., 1998), and (3) this species grows a large spherical chamber (Bé et al., 1973; Spero, 1988). The latter attribute is particularly advantageous because the final spherical chamber is massive (25–100 μg/shell), displays consistent geochemistry around its circumference (Fehrenbacher et al., 2015), and can be broken into chamber fragments for analysis without contamination from the juvenile chambers found in the earlier trochospiral part of the same shell. Thus, we measure $\Delta^{18}O_{SIMS-GSMS}$ values through analysis of identical foraminifer material using these two analytical techniques.

2. Materials and methods

2.1. Core-top specimens

Shells of *O. universa* were handpicked from the uppermost 3 cm of piston core CH15-PC9-00 (PC9) taken atop Blake Ridge (2790 m water depth; 31°55.691′N, 75°43.774′W) in the northwestern Atlantic (Fig. S1). Radiocarbon dating of this core-top sample has confirmed its

Holocene age (Wycech et al., 2016). The sample was disaggregated in a pH-buffered solution (pH ≈ 8) made of sodium hexametaphosphate, hydrogen peroxide (30 vol%), ammonium hydroxide, and distilled water, then rinsed with tap water over a 63-μm sieve. The resulting coarse fraction (> 63 μm) was subsequently rinsed with distilled water before being oven-dried (30 °C) overnight. The *O. universa* shells were handpicked from the > 355 μm sieve-size fraction.

The presence of aragonitic pteropod shells and dissolution-prone species of planktic foraminifers (i.e. *Globigerinoides ruber,* Berger, 1968, 1970; Adelseck Jr., 1978) possessing delicate spines indicates that the calcareous microfossil assemblage containing the *O. universa* shells experienced minimal carbonate dissolution. The surface textures of the *O. universa* shells were examined using back-scattered electron (BSE) imaging on a Hitachi S-3400 N scanning electron microscope (SEM) in variable pressure mode (Appendix B). The shells were not coated for BSE imaging. Each whole shell was then manually broken into smaller fragments using a surgical scalpel blade (e.g. Vetter et al., 2013). Whenever present, juvenile chambers were removed with one or two of the final chamber fragments being used for *in situ* $\delta^{18}O$ analyses by SIMS and the remaining fragments of the same final chamber being pooled for $\delta^{18}O$ analysis by GSMS (Fig. 1). Sample weights of pooled chamber fragments used for the GSMS analyses ranged from 10 to 90 μg. This "paired" approach allows us to make a direct comparison between the SIMS and GSMS $\delta^{18}O$ values obtained from the spherical, final chambers of a population of *O. universa* shells.

Three experiments were carried out to compare complementary SIMS and GSMS values for the PC9 *O. universa* shells. Shell fragments analyzed by SIMS and GSMS in each experiment were pre-treated in the same manner prior to final analytical preparation. In the first experiment, spherical chambers were not processed beyond picking the shells from the sample, cracking them open, and analyzing the calcite fragments. In the second experiment, the chamber fragments were cleaned for 10 min in a 1:1 solution of 30% hydrogen peroxide and 0.1 N sodium hydroxide at 65 °C to remove organic matter. The cleaned fragments were then rinsed with deionized water, sonicated for ~15 s in reagent grade methanol to remove material adhering to the surface of the fragments, and rinsed two additional times in deionized water. The third experiment entailed splitting the spherical chambers of each shell into three fragments; one fragment was analyzed by GSMS without treatment, while a second and third fragment were roasted *in vacuo* at 375 °C for 30 min to remove labile organic carbon and water. The two roasted fragments were subsequently used for analysis by GSMS and SIMS.

2.2. Cultured shells grown under controlled conditions

Paired SIMS-GSMS $\delta^{18}O$ analyses were also performed on eight *O. universa* shells grown in the laboratory. These shells were cultured in

1995 as part of a larger experiment described by Bemis et al. (1998) (Table S1). Specimens were maintained at constant temperature ($22 \pm 0.2\,°C$), $\delta^{18}O_{sw} = -0.25 \pm 0.05‰$ (VSMOW), salinity $= 33.3‰$, pH $= 8.04$, and with an ambient $[CO_3{}^{2-}]$ ($2250\,\mu mol\,kg^{-1}$). Many planktic foraminifer species, including *O. universa*, host algal symbionts whose photosynthetic activity enhances biocalcification and increases intra-shell $\delta^{18}O$ variability (Spero and Lea, 1993). The cultured specimens analyzed in this study were grown under varying light conditions, which increases inter-shell $\delta^{18}O$ variability. Five of the specimens were grown under a 12-h light:12-h dark cycle, two under low light intensity ($26–30\,\mu mol$ photons $m^{-2}\,s^{-1}$) and three under high light intensity ($400–700\,\mu mol$ photons $m^{-2}\,s^{-1}$). An additional three specimens were grown under continuous 24-h low light intensity. The spherical chambers of these cultured *O. universa* specimens calcified over a period of 3–9 days. The final spherical chamber of each specimen was cracked into fragments as described in Section 2.1 and then analyzed by GSMS and SIMS. The optical appearances and internal wall structures of the cultured *O. universa* shells were similar to those of shells recovered from the PC9 core-top (Appendix C).

2.3. In situ $\delta^{18}O$ measurement by SIMS

The *O. universa* chamber fragments and three grains of the UWC-3 calcite standard ($\delta^{18}O = -17.8‰$ VPDB; Kozdon et al., 2009) were placed within a 10-mm-diameter circle, cast in a 25-mm-diameter epoxy mount, ground to the level of best exposure in cross-section, polished with carbonate-epoxy relief of less than $\sim1\,\mu m$ (Kita et al., 2009), cleaned, and gold coated. Secondary electron (SE) SEM images of each mounted shell fragment were taken in high-vacuum mode to assess the quality of sample exposure and cross-section geometry prior to SIMS analysis.

In situ $\delta^{18}O$ analyses were performed with a CAMECA IMS 1280 ion microprobe (SIMS) at the WiscSIMS Laboratory, Department of Geoscience, University of Wisconsin-Madison using a $^{133}Cs^+$ primary ion beam. Each series of 8–12 measurements of foraminifer calcite $\delta^{18}O$ was bracketed by 4–6 consecutive $\delta^{18}O$ analyses (both before and after) of a UWC-3 standard grain in the center of the sample mount. The 8 or more bracketing analyses were used to determine calcite instrumental mass fractionation corrections and calculate the spot-to-spot reproducibility (2 SD) for each set of foraminifer measurements. SIMS $\delta^{18}O$ values are reported in reference to VPDB. After analysis, each SIMS pit was individually imaged (Appendix B) and examined by SEM using the SE detector in high vacuum mode (see Section S1, Fig. S2). SIMS pits intersecting cracks and/or epoxy were omitted from further interpretation. Raw and final processed data are reported in Tables S2–S4.

For 10-μm SIMS spots (~1-μm deep) the primary ion beam intensity was ~1.2 nA, comparable to Kozdon et al. (2013). The resulting secondary $^{18}O^-$, $^{16}O^-$, and $^{16}OH^-$ ions were detected simultaneously from the 10-μm spots using three Faraday cup detectors with a typical $^{16}O^-$ count rate of 2.3×10^9 counts per second (cps). The energy slit width for secondary ions was 40 eV, which was re-centered during tuning for each analytical session. Simultaneous measurement of $^{16}OH^-$ with $^{16}O^-$ and $^{18}O^-$ during SIMS analysis provides $^{16}OH^-/^{16}O^-$ ratios (OH/O hereafter), which are used to gauge the relative hydrogen content in the sample, likely in the form of water and/or organic matter. Even at ultra-high vacuum, the analytical chamber of the SIMS contains detectable hydrous compounds, so the reported OH/O ratios were background-corrected by subtracting the average OH/O of the UWC-3 (nominally anhydrous metamorphic calcite) bracketing data from the OH/O ratio of the foraminifer. In addition to pit appearance, the OH/O ratio, $^{16}O^-$ count rate, and secondary ion yield (cps/nA) relative to the mean of the bracketing standard analyses served as a basis for assessing the quality of each intervening sample measurement (see Section S1). The total analytical time per spot was ~3 min for 10-μm spots including pre-sputtering. The average

external precision (spot-to-spot reproducibility) for the 10-μm analyses, reported as two times the standard deviation of the bracketing standard measurements, was $\pm 0.3‰$ (± 2 SD). A total of 160 SIMS measurements using 10-μm spots were performed on *O. universa* chamber fragments in addition to 93 bracketing measurements of the UWC-3 standard.

A second analytical setup with a primary-beam current of 19–21 pA and a spot size of ~3-μm (~1-μm deep) was used to investigate intra-chamber $\delta^{18}O$ variability (i.e. potential $\delta^{18}O$ variation during ontogenetic chamber thickening) and measure thin-walled *O. universa* shells from PC9 (e.g. Kozdon et al., 2009; Vetter et al., 2013). Secondary $^{18}O^-$, $^{16}O^-$, and $^{16}OH^-$ ions were detected simultaneously using an electron multiplier ($^{18}O^-$) and two Faraday cups ($^{16}O^-$, $^{16}OH^-$) with a mean $^{16}O^-$ count rate of 3.3×10^7 cps. The energy slit width for secondary ions was 40 eV for 3-μm $\delta^{18}O$ analyses, and was re-centered during tuning for each analytical session. The electron multiplier deadtime correction was 68 ns. In addition to pit appearance and OH/O, the $^{16}O^-$ count rate relative to the mean of the bracketing standard analyses served as a basis for assessing the quality of each $\delta^{18}O$ measurement (see Section S1). Prior to the November 2015 session, the electron multiplier gain was monitored before the third analysis of each group of UWC-3 standard analyses and, when necessary, the high voltage applied to the detector was increased by 1–6 V to compensate for drift in the electron multiplier gain. A new, permanent protocol for gain adjustment was implemented during the November 2015 session, such that the electron multiplier gain was monitored after each analysis and adjusted automatically as needed at a rate of 3–5 V per hour. The total analytical time was ~7 min per 3-μm spot. The average precision (reproducibility on UWC-3) for the 3-μm analyses was $\pm 0.7‰$ (± 2 SD, spot-to-spot). A total of 140 SIMS measurements using 3-μm spots were performed on *O. universa* chambers in addition to 93 bracketing measurements of the UWC-3 standard. The 3-μm analyses include the measurement of several spherical *O. universa* chambers from PC9 (untreated, $n = 6$ shells) and culture ($n = 4$ shells) that were also measured by 10-μm SIMS spots. Use of a smaller beam spot size (3-μm) made it possible to carry out SIMS $\delta^{18}O$ analyses on an additional 16 *O. universa* shells possessing thin-walled ($< 10\,\mu m$) chambers.

2.4. $\delta^{18}O$ measurement by gas source mass spectrometry

Untreated and cleaned chamber fragments of *O. universa* shells from the PC9 core-top sample were analyzed at the University of California, Santa Cruz (UCSC) using a ThermoScientific Kiel IV carbonate device interfaced to a ThermoScientific MAT-253 dual-inlet isotope ratio mass spectrometer. The foraminifer fragments were digested in concentrated phosphoric acid (specific gravity $= 1.92$ g/mL; Coplen et al., 1983) at 75 °C. The external analytical precision is $\pm 0.1‰$ (2 SD) for the $\delta^{18}O$ measurement of fragmented foraminifer samples weighing 10–90 μg.

The $\delta^{18}O$ compositions of chamber fragments from cultured *O. universa* shells, as well as roasted chamber fragments of *O. universa* shells from the PC9 core-top, were measured at the University of California, Davis (UCD) using a Fisons Optima isotope ratio mass spectrometer fitted with a common acid bath auto-carbonate device. The foraminifer fragments were digested in concentrated phosphoric acid (specific gravity $= 1.92$ g/mL; Coplen et al., 1983) at 90 °C, and corrected for acid digestion fractionation by paired measurement with a Carrara marble standard that was previously calibrated against NBS-19. External analytical precision is $\pm 0.1‰$ (2 SD) for $\delta^{18}O$ in the fragmented foraminifer samples weighing 10–90 μg. Foraminifer sample weights were comparable between the GSMS analyses completed in the UCSC and UCD laboratories.

For comparative purposes, three samples of the UWC-3 standard were analyzed by GSMS at both UCSC and UCD. For the analyses at UCSC, each sample weighed 73–91 μg and was composed of 2–5 calcite grains. At UCD, each sample was composed of a single grain that weighed 31–40 μg. The GSMS $\delta^{18}O$ values measured from the UWC-3

Table 1

GSMS $\delta^{18}O$ values for UWC-3 calcite. Measurements performed at the University of Wisconsin-Madison previously reported in Kozdon et al. (2009).

Laboratory	Number of grains per analysis	Number of analyses	Sample weight (µg)	$\delta^{18}O$ (‰, VPDB)		
				Average	2 SD	2 SE
University of Wisconsin-Madison	1–10	9	4000–8000	−17.8	0.1	0.1
University of California-Santa Cruz	2–5	3	73–91	−17.9	0.3	0.2
University of California-Davis	1	3	31–40	−17.8	0.2	0.1

* Accepted value for $\delta^{18}O$ (UWC-3) is −17.8 ± 0.1‰ (VPDB) (Kozdon et al., 2009).

standard at UCSC and UCD were subsequently compared to those of UWC-3 previously measured by GSMS at the University of Wisconsin-Madison (Kozdon et al., 2009).

3. Results

3.1. Comparison of paired SIMS-GSMS $\delta^{18}O$ analyses

The $\delta^{18}O$ measurement of foraminifer calcite by SIMS is standardized to the GSMS-derived $\delta^{18}O$ value of the UWC-3 calcite standard. For this reason, we first analyzed the UWC-3 standard by GSMS in the same laboratories that measured the foraminifer fragments. GSMS $\delta^{18}O$ values (relative to VPDB) of UWC-3 analyzed by UCSC (−17.9 ± 0.2, 2SE) and UCD (−17.8 ± 0.1) are within analytical precision of the GSMS-derived published value (−17.8 ± 0.1‰, Kozdon et al., 2009) used for instrumental correction of the raw SIMS data (Table 1). We note that the GSMS measurements of UWC-3 carried out at UCSC and UCD were of a comparable size to fragmented foraminifer chambers (30–40 µg), and reproduced the established UWC-3 $\delta^{18}O$ value within 0.1‰.

The differing spatial resolutions (3 µm vs. 200 µm), weights (10^{-5} µg vs. 10 µg), and volumes (10 µm^3 vs. 10^7 µm^3) of material analyzed by SIMS and GSMS techniques necessitate thorough investigation of the intra-shell $\delta^{18}O$ variability captured by SIMS. Hence, $\delta^{18}O$ profiles were generated across final chamber fragments using a series of 3-µm SIMS analyses (Fig. 2). The $\delta^{18}O$ values measured along each transect are within analytical uncertainty; hence, no consistent trends or patterns emerge from the series of 3-µm SIMS $\delta^{18}O$ measurements taken across the final chamber walls of the *O. universa* shells (n = 15) collected from the PC9 core-top (Fig. 2). Consequently, the mean SIMS $\delta^{18}O$ value of each chamber was used for comparison to the paired GSMS $\delta^{18}O$ value.

The 3-µm and 10-µm SIMS analyses use different instrument settings with different levels of analytical precision. Thus, $\delta^{18}O$ measurements using both the 3-µm and 10-µm spots were conducted on the spherical chambers of several *O. universa* shells from the PC9 core-top (untreated, n = 6 shells) and culture experiments (n = 4 shells) (Fig. 3, Table 2). The 3-µm and 10-µm SIMS measurements from the same shells have comparable $^{16}O^-$ count rate ratios (foraminifer/bracketing standard = 0.92–1.03) and background-corrected OH/O ratios (0.006–0.010). Although the 3-µm analyses are less precise relative to the 10-µm analyses, the 3-µm and 10-µm $\delta^{18}O$ values measured from the same PC9 chambers are indistinguishable (unpaired *t*-test *p*-value of 0.928, Fig. 3A). Moreover, the 3-µm and 10-µm SIMS $\delta^{18}O$ data measured from all untreated shells taken from the PC9 core-top sample are statistically identical (unpaired t-test p-value of 0.52) (Fig. S3, Table S5). By contrast, the mean 3-µm $\delta^{18}O$ values for the cultured shells are, on average, 0.6 ± 0.6‰ (± 2 SE) lower than those of mean 10-µm $\delta^{18}O$ values from the same shell (Fig. 3B). An unpaired t-test on the individual 10-µm and 3-µm SIMS $\delta^{18}O$ values indicates that the $\delta^{18}O$

difference measured among the cultured shells is statistically significant at the 95% confidence level. This difference between the SIMS $\delta^{18}O$ values acquired from 3-µm and 10-µm analysis pits in the cultured shells (Fig. 3B) led us to evaluate these two datasets separately in order to more thoroughly document possible inter-instrument differences.

We observe a consistent $\Delta^{18}O_{SIMS\text{-}GSMS}$ offset of −0.7 to −1.0‰ in all methodological comparison experiments (Table 3). The $\Delta^{18}O_{SIMS\text{-}GSMS}$ values were calculated for each spherical chamber to produce a dataset of per shell $\Delta^{18}O_{SIMS\text{-}GSMS}$ values that were averaged for each experiment. The inter-instrument $\delta^{18}O$ differences are shown in Fig. 4 where the paired SIMS-GSMS values consistently fall below the theoretical 1-to-1 lines. The SIMS-GSMS $\delta^{18}O$ differences are not statistically different between experiments (Table 3), and the entire paired dataset has an average $\Delta^{18}O_{SIMS\text{-}GSMS}$ value of −0.9 ± 0.1‰ (± 2 SE, n = 66 pairs; Fig. 4F). A salient aspect of the paired $\delta^{18}O$ data is the positive correlation between SIMS and GSMS values over the ~3‰ range of $\delta^{18}O$ values measured from different *O. universa* spherical chambers (Fig. 4).

Although the $\Delta^{18}O_{SIMS\text{-}GSMS}$ values between experimental groups are similar, roasting and cleaning by sonication and hydrogen peroxide may have a larger effect on $\delta^{18}O$ values measured by one analytical technique. As a consequence, the effects of shell treatment on SIMS and GSMS $\delta^{18}O$ values are investigated separately (see Section S2, Figs. S3-S4, Table S5). Comparison of SIMS and GSMS $\delta^{18}O$ values of untreated and treated (cleaned, roasted) shells by a *t*-test indicates that treatment does not have an appreciable effect on $\delta^{18}O$ values measured by either analytical technique (Figs. S3-S4, Table S5 p-values). This inference is based on the comparison of "unpaired" values measured for the suite of shells in the untreated and roasted experiments, which register a large degree of inter-shell $\delta^{18}O$ variability (~2–3‰) (Figs. S3-S4). Paired GSMS $\delta^{18}O$ analyses of roasted and unroasted fragments of the same chamber remove uncertainties related to inter-shell variability, and indicate that roasting decreases GSMS $\delta^{18}O$ values by 0.1‰ on average (Fig. 5, Table S7). The paired roasted-unroasted GSMS $\delta^{18}O$ difference is small, but statistically significant (paired t-test p-value = 0.0015).

3.2. SIMS-GSMS $\delta^{18}O$ differences

The positive correlation and strong covariance between the SIMS and GSMS $\delta^{18}O$ values raises the prospect that a simple correction or "adjustment factor" may be appropriate for bringing the two datasets into agreement. Thus, the average $\Delta^{18}O_{SIMS\text{-}GSMS}$ value of 0.9‰ was added uniformly to the measured SIMS $\delta^{18}O$ values. We opted to adjust the SIMS values because GSMS has been the established technique for measuring isotope ratios in carbonates for nearly seven decades (e.g. McCrea, 1950; Epstein et al., 1953) and a majority of published data have been measured by GSMS. We note, however, that the offset between $\delta^{18}O_{GSMS}$ and $\delta^{18}O_{SIMS}$ values likely results from a complex combination of factors that affect the $\delta^{18}O$ values generated by the two techniques (see Section 4). The uniform adjustment made to the SIMS $\delta^{18}O$ values measured in the multiple experimental groups effectively removes the inter-instrument differences as reflected by the excellent agreement between the data and theoretical 1-to-1 lines (Fig. 6).

4. Discussion

Although the SIMS $\delta^{18}O$ values are offset from the paired GSMS values, the strong positive covariance between the two datasets over a 2–3‰ $\delta^{18}O$ range (Fig. 4) indicates that both analytical techniques record environmental changes that contributed to inter-shell $\delta^{18}O$ variation such as temperature, $\delta^{18}O_{sw}$ (Bemis et al., 1998) and physiological processes that affect microenvironment carbonate chemistry (Spero et al., 1997). Furthermore, the consistent ~0.9‰ $\Delta^{18}O_{SIMS\text{-}GSMS}$ value measured in each experiment allays concerns regarding sample treatment, and simplifies the proposed adjustment to SIMS $\delta^{18}O$ values measured from geologically young (Quaternary) *O. universa* shells. However, we caution that such an adjustment to SIMS $\delta^{18}O$ values
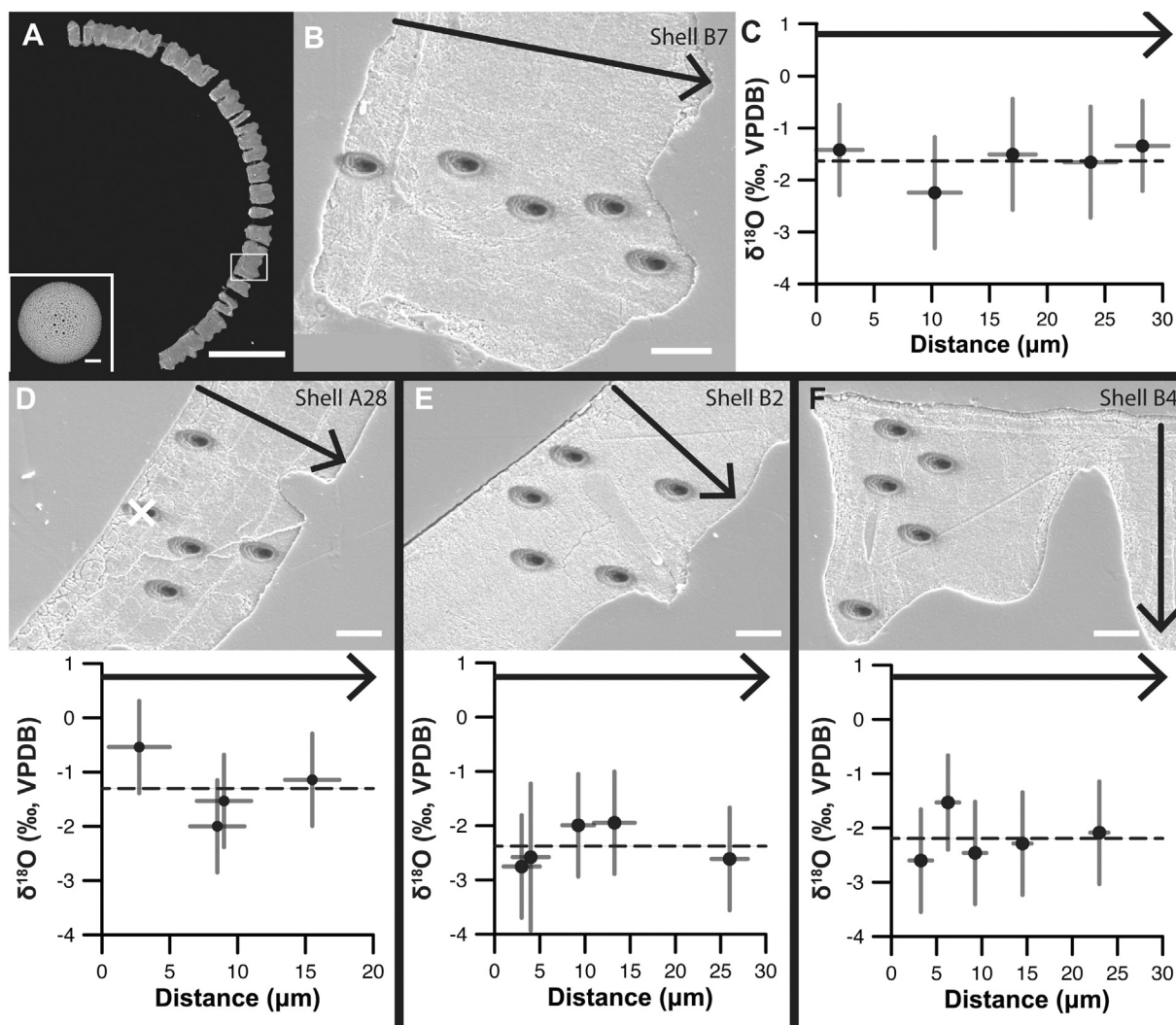
Fig. 2. SEM images showing final chamber fragments of *O. universa* in cross-section with transects of 3-μm SIMS analysis pits and their corresponding $\delta^{18}O$ values (error bars: horizontal = width of SIMS pits, vertical = analytical precision, 2 SD). All chamber fragments shown are from PC9 core-top specimens, arrows point toward chamber wall exterior, and dashed lines extending across plotted $\delta^{18}O$ data denote mean value for each chamber fragment. Results are representative of 3-μm and 10-μm SIMS spot analyses. A. Cross-section of chamber fragment cast in epoxy (black) with original whole shell in inset (scale bars = 100 μm). Box overlain on chamber cross-section delimits area of SIMS transect shown in B. B. Transect of SIMS pits across cross-section of chamber wall shown in A (scale bar = 5 μm). C. $\delta^{18}O$ values for SIMS pits shown in B plotted against distance from chamber wall interior. D-F. Upper panels showing transects of SIMS analysis pits running across cross-sections of chamber walls (scale bars = 5 μm), lower panels show corresponding $\delta^{18}O$ values plotted against distance from chamber wall interior.

acquired from shells belonging to foraminifer taxa possessing differing microcrystalline structures, chemistries, and/or preservation histories, is a matter of ongoing testing. We also note that the adjustment herein proposed may not be appropriate for *in situ* $\delta^{18}O$ analyses carried out on foraminifer shells at other SIMS facilities since standards and operating conditions can vary.

4.1. SIMS-GSMS $\delta^{18}O$ difference

The inter-instrument differences reported in this study may arise from both GSMS analyses entailing acid digestion of whole shells and *in situ* SIMS analyses that subsample micrometer-scaled domains within an individual shell. Differences in paired SIMS-GSMS $\delta^{18}O$
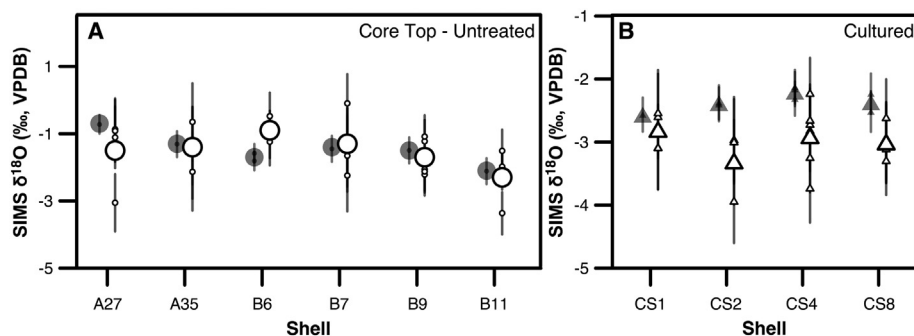

Fig. 3. Comparison of intra-chamber $\delta^{18}O$ values measured with 3-μm and 10-μm SIMS analysis pits in *O. universa* chambers. A. Untreated chamber fragments of shells from PC9 core-top, B. cleaned chamber fragments of cultured shells. Labels along abscissa are the whole shell ID numbers (see Appendix B). Individual analyses (small symbols) are from 3-μm pits (open symbols) and 10-μm pits (filled symbols) with average $\delta^{18}O$ values per shell (large symbols). Error bars are external precision on individual SIMS $\delta^{18}O$ values (± 2 SD).

Table 2
Average SIMS $\delta^{18}O$ values ($\pm$ 2SE) measured by 3-µm and 10-µm pits in *O. universa* shells collected from the PC9 core-top (untreated) and grown in culture as shown in Fig. 3.

Sample	Whole Shell ID	3 µm		10 µm	
		Average $\delta^{18}O$ (‰, VPDB)	n	Average $\delta^{18}O$ (‰, VPDB)	n
PC9 Core-Top (untreated)	A27	−1.5 ± 1.1	4	−0.7 ± 0.3	1
	A35	−1.4 ± 0.6	4	−1.3 ± 0.4	1
	B6	−0.9 ± 0.5	3	−1.7 ± 0.2	2
	B7	−1.3 ± 0.4	9	−1.4 ± 0.4	1
	B9	−1.7 ± 0.5	5	−1.5 ± 0.4	1
	B11	−2.3 ± 0.8	4	−2.1 ± 0.4	1
Culture	CS1	−2.8 ± 0.3	4	−2.6 ± 0.3	1
	CS2	−3.3 ± 0.5	4	−2.4 ± 0.0	2
	CS4	−2.9 ± 0.4	7	−2.2 ± 0.1	3
	CS8	−3.0 ± 0.2	7	−2.4 ± 0.3	2

measurements of biogenic carbonates and speleothems have been previously reported, but the magnitude of the difference appears to vary with investigative procedures and the type of carbonate analyzed (Treble et al., 2007; Hanson et al., 2010; Allison et al., 2010; Orland, 2012; Liu et al., 2015; Orland et al., 2015). Such comparisons of SIMS and GSMS $\delta^{18}O$ values have revealed correlations to mineralogy (calcite, aragonite), sample age, and OH/O (Orland et al., 2015). Although existing empirical $\delta^{18}O$-temperature calibrations are based on GSMS measurements, neither SIMS nor GSMS $\delta^{18}O$ values should be regarded, a priori, as being more accurate. Furthermore, it is noted that SIMS analyses entail the isolated measurement of micrometer-scale targets, which permits the operator to avoid irregular or altered appearing domains. Thus, the mean SIMS $\delta^{18}O$ value of each chamber may be restricted to specific sub-domains of a test and not represent the bulk $\delta^{18}O$ composition of larger samples measured by GSMS.

4.2. GSMS caveats

GSMS is the primary technique used for $\delta^{18}O$ measurement of foraminiferal calcite. In the past, problems with these conventional analyses were attributed to inter-lab calibration, gas leaks, incomplete acid digestion of the sample, surface area differences between the sample and standard (sensu Wacker et al., 2013), analysis of water or organics (Oehlerich et al., 2013), or sample-reference gas misbalance (Potts, 1992; Wright, 1998). The two GSMS laboratories that analyzed *O. universa* chambers reproduced the $\delta^{18}O$ value of the UWC-3 calcite standard within 0.1‰ of the published value obtained at University of Wisconsin (Kozdon et al., 2009) even though the measurements were performed using different acid-digestion temperatures, sample sizes, and instrumental set-ups (Kiel device at 70 °C versus common acid bath at 90 °C). On the other hand, foraminifer sample treatment in this study does appear to have a minor effect on the $\delta^{18}O$ value measured by the acid-digestion technique given that *in vacuo* roasting of *O. universa* fragments decrease GSMS $\delta^{18}O$ values by 0.1‰ on average (Fig. 5, Table S7). Overall, the results of the UWC-3 analyses and the roasting experiment suggest that < 30% of the measured 0.9‰ SIMS-GSMS $\delta^{18}O$ difference can be attributed to analytical aspects of the GSMS analyses. Below, we evaluate other explanations for the SIMS-GSMS $\delta^{18}O$ differences herein documented.

4.3. Potential causes of $\Delta^{18}O_{SIMS-GSMS}$

4.3.1. Matrix effects

Stable isotope analysis by SIMS is a comparative technique and requires a reference material that matches the sample in mineralogy, chemical composition, and microcrystalline texture (Valley and Kita, 2009; Śliwiński et al., 2016). The biogenic processes by which foraminifers precipitate their shells (e.g. de Nooijer et al., 2014) are

Table 3
Summary of paired SIMS and GSMS $\delta^{18}O$ measurements of untreated, cleaned, and roasted chambers from PC9 core-top (0-3 cm) and the cleaned cultured chambers.

SIMS Spot Size	Sample	Description	n	Average SIMS $\delta^{18}O$ (‰, VPDB)	Average GSMS $\delta^{18}O$ (‰, VPDB)	$\Delta^{18}O_{SIMS-GSMS}$ (‰)	SIMS vs GSMS $\delta^{18}O$ p-value	$\Delta^{18}O_{SIMS-GSMS}$ Untreated-Treated p-value	Average $^{16}OH/^{16}O$
3-µm	PC9	Untreated	15	−1.7 ± 0.4	−0.7 ± 0.4	−1.0 ± 0.2	3.7×10^{-8}[a]	0.14	$(12.1 \pm 3.1) \times 10^{-3}$
10-µm	PC9	Untreated	11	−1.6 ± 0.3	−0.8 ± 0.2	−0.8 ± 0.2	3.3×10^{-5}[a]	NA	$(9.4 \pm 0.6) \times 10^{-3}$
	PC9	Hydrogen Peroxide Cleaned, Sonicated	15	−1.7 ± 0.2	−0.8 ± 0.2	−0.9 ± 0.1	7.2×10^{-10}[a]	0.52	$(9.6 \pm 0.3) \times 10^{-3}$
	PC9	Roasted	13	−1.3 ± 0.5	−0.6 ± 0.4	−0.7 ± 0.2	1.2×10^{-5}[a]	0.82	$(1.4 \pm 0.4) \times 10^{-3}$
	Culture	Hydrogen Peroxide Cleaned	8	−2.4 ± 0.1	−1.7 ± 0.2	−0.7 ± 0.1	4.8×10^{-6}[a]	0.72	$(8.7 \pm 0.8) \times 10^{-3}$

Number of shells (n) analyzed in each experimental group. Average SIMS and GSMS $\delta^{18}O$ values used to calculate $\Delta^{18}O_{SIMS-GSMS}$ ($\pm$ 2 SE). The $\Delta^{18}O_{SIMS-GSMS}$ values of untreated (10-µm pits) and treated shells are significantly different when p-values are < 0.05. Background-corrected OH/O ratios ($\pm$ 2 SE).
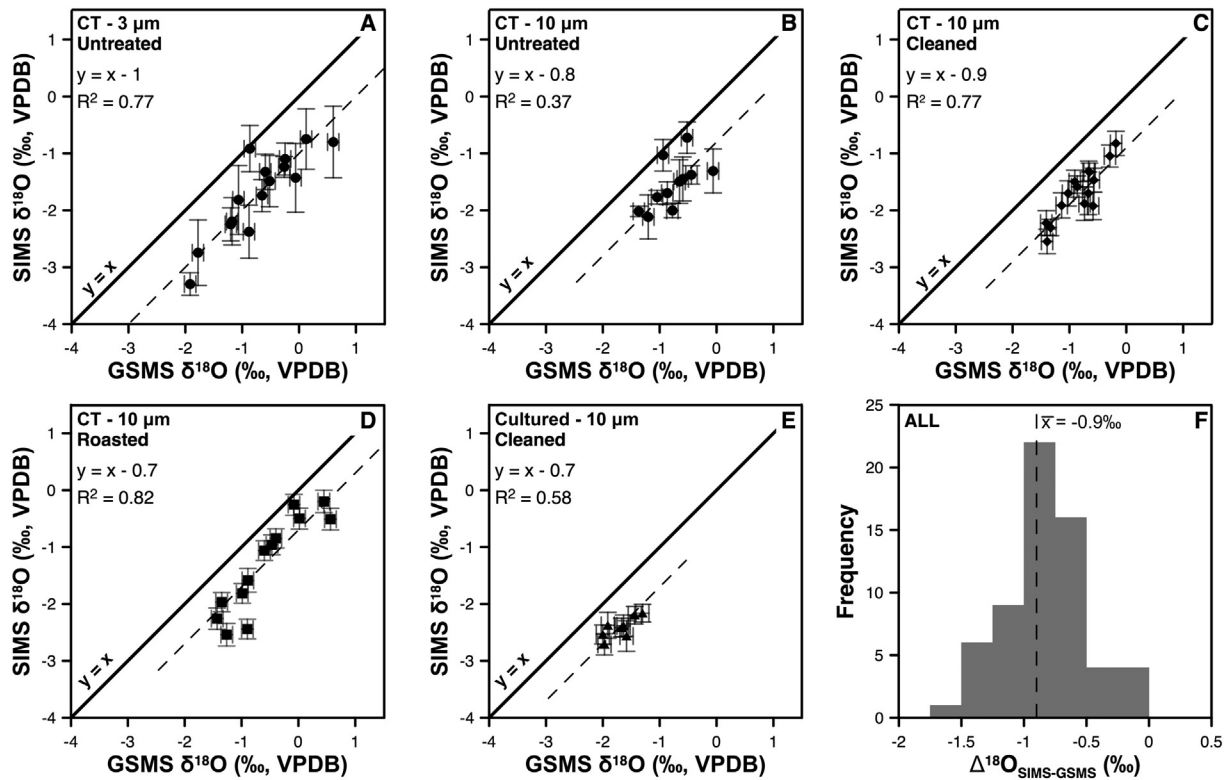[a] Difference is statistically significant.

Fig. 4. Comparison of paired SIMS and GSMS δ18O values from the same chamber of *O. universa* shells. Theoretical 1-to-1 lines (solid bold lines) denote no difference between corresponding SIMS and GSMS δ18O values. Linear regression with slope = 1 (dashed lines) fit to data. A. Untreated core-top shells (3-μm SIMS analyses), B. untreated core-top shells (10-μm SIMS analyses), C. cleaned core-top shells (10-μm SIMS analyses), D. roasted core-top shells (10-μm SIMS analyses), and E. cleaned shells from culture experiment (10-μm SIMS analyses). All SIMS data shown are average chamber values. Error bars are GSMS analytical precision (± 2 SD, horizontal) and propagated error from multiple SIMS measurements per shell (± 2 SE, vertical). F. Histogram of $\Delta^{18}O_{SIMS-GSMS}$ values for the paired datasets in A-E. Average $\Delta^{18}O_{SIMS-GSMS}$ value (dashed vertical line).
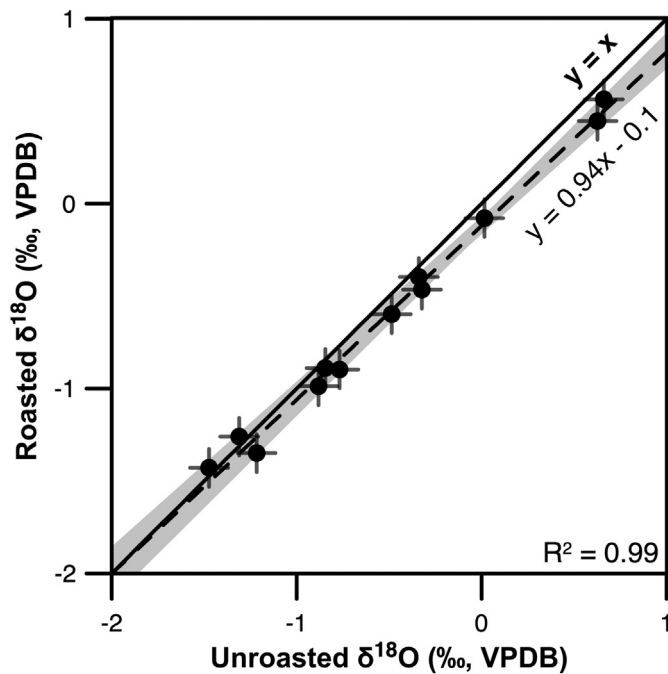

Fig. 5. Comparison of GSMS δ18O values measured from unroasted and roasted fragments of the same *O. universa* shell. Robust regression using iteratively reweighted least squares (dashed line) with corresponding slope (m) and y-intercept (b). 95% confidence interval on the slope (0.89 to 0.99) and y-intercept (−0.2 to −0.1) (grey shading). R^2 from unweighted least squares regression. Theoretical 1-to-1 line denoting no difference (solid line). Error bars express external instrumental precision (± 2 SD).

fundamentally different from the recrystallization that occurs in a granulite facies marble that formed the UWC-3 standard. This is noteworthy because these abiotic/biotic processes give rise to carbonates with different microstructures and chemistries, and the SIMS analyses performed in this study were standardized with the assumption that the instrumental mass fractionation (IMF) of the UWC-3 analyses matches that of the samples. Such an assumption may be overly simplistic.

SIMS and GSMS analyses assume the analyzed foraminifers have calcite mineralogy. However, a small component (≤4.5%) of *O. universa* shells may be composed of the unstable calcium carbonate polymorph, vaterite (Jacob et al., 2017), which has a SIMS IMF and GSMS acid-fractionation factor that might differ from calcite (Kim and O'Neil, 1997). Yet, preservation of foraminifer vaterite by SIMS and/or GSMS is an unlikely explanation for the $\Delta^{18}O_{SIMS-GSMS}$ values in this study due to the significant amount of time elapsed between calcification and analysis (i.e., 20 years for cultured shells, ~1870 years for core-top shells).

The microcrystalline texture of foraminifer shells could also affect IMF thereby causing differences between SIMS δ18O analyses of biogenic carbonate samples and a standard that crystallized at high temperatures. Such an issue is evidenced by previous SIMS analyses and SEM imaging of nautiloid shells, which reveal that more porous domains yield δ18O values ~0.8‰ lower than those of less porous, neighboring domains in the same shell (Linzmeier et al., 2016). Furthermore, foraminifer δ18O values measured with SIMS may be affected by oxygen-bearing contaminant phases such as water or organics that have isotope ratios, IMF, and/or SIMS oxygen-ionisation probabilities that differ from calcite. The OH/O ratios measured from *O. universa* chambers in this study indicate that the foraminifer matrix contains a hydrogen-bearing phase that was partly removed by vacuum roasting (Fig. 7).

Given our current understanding, a mismatch between the UWC-3 standard and the foraminifer matrix is likely a major source of the
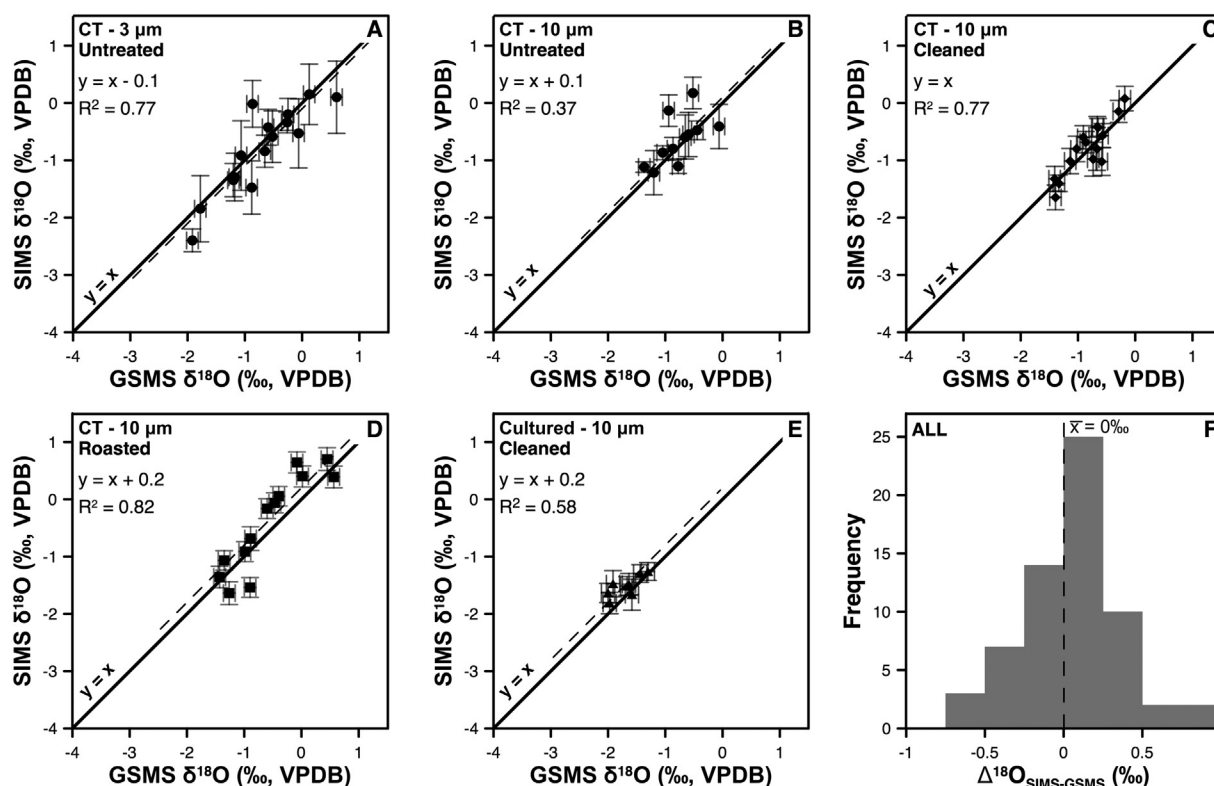
Fig. 6. Adjusted (+0.9‰) SIMS $\delta^{18}O$ values plotted against GSMS $\delta^{18}O$ values from the same chamber of *O. universa* shells. Theoretical 1-to-1 line (solid bold line) denotes no SIMS-GSMS $\delta^{18}O$ difference. Linear regression with slope = 1 (dashed lines) fit to data. A. Untreated core-top shells (3-μm SIMS analyses), B. untreated core-top shells (10-μm SIMS analyses), C. cleaned core-top shells (10-μm SIMS analyses), D. roasted core-top shells (10-μm SIMS analyses), and E. cleaned shells from culture experiment (10-μm SIMS analyses). All SIMS data shown are average chamber values, and have been adjusted (see Section 3.2). Error bars are GSMS analytical precision (±2 SD, horizontal) and propagated error from SIMS measurements (±2 SD, vertical). F. Histogram of adjusted $\Delta^{18}O_{SIMS-GSMS}$ values for the paired datasets in A-E. Average adjusted $\Delta^{18}O_{SIMS-GSMS}$ value (dashed vertical line).

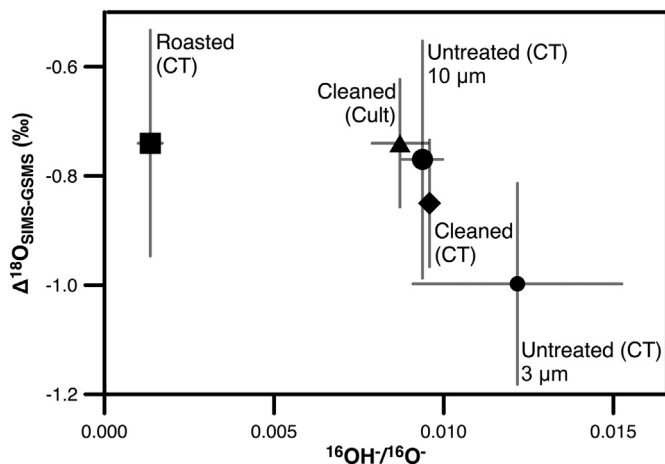**Fig. 7.** Average $\Delta^{18}O_{SIMS-GSMS}$ values plotted against background-corrected OH/O ratios measured for *O. universa* chambers that were untreated (circles), cleaned with hydrogen peroxide and sonication (diamond), and roasted (square) from the Site PC9 core-top (CT), and for cultured (Cult) *O. universa* chambers cleaned with hydrogen peroxide (triangle). Note: $\Delta^{18}O_{SIMS-GSMS}$ for untreated chambers measured using 10-μm (large circle) and 3-μm (small circle) SIMS pits. Error bars are 2 times the standard error of the OH/O ratio mean (horizontal) and the $\Delta^{18}O_{SIMS-GSMS}$ mean (vertical).

SIMS-GSMS $\delta^{18}O$ difference reported in all experimental iterations of this study. Unfortunately, identifying a homogeneous calcite standard that is perfectly matched to foraminifer shells for SIMS analysis is challenging due to the natural variability and complex mechanisms of biogenic calcification. With the possibility of a standard-sample mismatch in mind, we consider other matrix-related factors such as differences in minor element composition, crystal size, the presence of

Table 4
Minor element composition of the UWC-3 standard and *O. universa* calcite.

Element	Concentration (ppmw)		*O. universa* References
	UWC-3	*O. universa*	
Mg	5457	243–4127	Boyle, 1981; Carpenter and Lohmann, 1992; Delaney et al., 1985; Eggins et al., 2004; Lea et al., 1999; Russell et al., 2004; Sadekov et al., 2005; Spero et al., 2015
Fe	4046	95–323	Boyle, 1981
Sr	2227	1050–1576	Carpenter and Lohmann, 1992; Delaney et al., 1985; Lea et al., 1999; Russell et al., 2004; Bender et al., 1975
Mn	1222	37–40	Boyle, 1981
Ba	1234	1.1–5.5	Lea et al., 1999; Lea and Boyle, 1991

Element composition of UWC-3 previously reported in Kozdon et al. (2009). *O. universa* shells analyzed in previous studies were either grown in laboratory culture or recovered from pelagic sediments.

water and organic matter, or high-$\delta^{18}O$ domains in foraminifers that are selectively avoided by SIMS. These effects are discussed below.

4.3.2. Cation composition and matrix effects

The importance of cation composition for correcting matrix effects on SIMS analyses in carbonates has long been known (Eiler et al., 1997, 2002; Valley and Kita, 2009), and it has recently been shown that minor Fe concentrations can have a large effect on carbonate IMF (Śliwiński et al., 2016, 2017). These studies indicate that minor- and possibly trace-element compositions of calcite (i.e., Mg, Fe, Mn, Sr, Ba) need to be examined in more detail for their effect on carbonate IMF. We note that the UWC-3 calcite standard has higher concentrations of these elements than are published for *O. universa* (Table 4). Analysis of newly

calibrated inorganic calcite standards indicates that the chemical compositions for *O. universa* in Table 4 cause systematic differences in IMF, and correcting for these differences would raise the sample $\delta^{18}O$ values reported here by 0.3–0.7‰ (Śliwiński et al., 2016, 2017; Sliwinski and Kitajima, pers. comm., Feb. 2018). Thus, IMF differences attributed to minor- and trace-element content of *O. universa* vs. UWC-3 may be a major cause of the $\Delta^{18}O_{SIMS-GSMS}$ values herein reported; however, a more detailed correction is beyond the scope of the present study because IMF values can change from session to session and thus calibration standards must be run at the same time as samples. At the time of this study, the new calcite standards had not been calibrated, and so neither the IMF of the new standards or the minor element compositions of *O. universa* were analyzed. Future studies will evaluate the importance of minor element substitutions for SIMS analysis of calcite in more detail.

4.3.3. SIMS measurement of matrix-bound organics

SIMS $\delta^{18}O$ analysis involves the measurement of all oxygen-bearing phases in the excavated SIMS pit, which includes organic matter, water, and/or sulfate. These shell components are not thought to contribute to the CO_2 analyzed by GSMS during phosphoric acid digestion. Thus, SIMS measurement of biogenic carbonates will be affected if organics are present in the volume of the SIMS pit. Organic matter could form inclusions, be bound within the calcite matrix (Spero, 1988), or occur as nano-phases along grain boundaries (Cuif et al., 2012). Relatively young (modern to Miocene-aged) foraminifer shells are composed of 0.02–0.2% organics, typically amino acids and proteins that contain up to 25% oxygen (King Jr and Hare, 1972; Robbins and Brew, 1990).

The cleaning and sonication treatment was performed to remove shell organics in *O. universa*, and the roasting experiment was performed to remove labile organic compounds and associated hydrated phases, while leaving refractory compounds within the matrix. Organics in biogenic carbonates are typically distributed throughout the mineral matrix in inter- and intra-crystalline voids, and have proven difficult to remove even with extreme cleaning techniques such as powdering and bleaching (Gaffey, 1990; Ren et al., 2009). The refractory nature of such organics is evidenced by the retention of a primary $^{15}N/^{14}N$ geochemical signal in 212 Ma Triassic corals (Frankowiak et al., 2016). These observations are further supported by the fact that our hydrogen peroxide cleaning procedure had no discernible effect on either the SIMS or GSMS $\delta^{18}O$ values (Figs. S3-S4, Tables 3, S5).

Direct comparison of GSMS $\delta^{18}O$ values measured from untreated and roasted fragments of the same *O. universa* shell chamber yields an offset range of 0.1 to −0.2‰ (Table S7) with an average decrease in $\delta^{18}O$ for roasted samples of 0.1 ± 0.1‰ (2 SD; Fig. 5). However, we note that the fragments looked grey in color after roasting, evidence of organic carbon maturation. This observation implies reaction, but ineffective removal of refractory organic contaminants. Still, the roasted chambers ($n = 13$) have lower OH/O ratios than the untreated, cleaned, and cultured chambers, indicating that a portion of the water and/or volatile organic contaminants are removed by roasting (Fig. 7). The lower GSMS $\delta^{18}O$ values registered by the roasted fragments are consistent with data from previous experiments in which GSMS $\delta^{18}O$ values of crushed, vacuum-roasted foraminifers are 0–0.5‰ lower than the $\delta^{18}O$ values of crushed unroasted foraminifers (e.g. Emiliani, 1966; Erez and Honjo, 1981). These earlier studies compared only a few roasted and unroasted samples that were comprised of hundreds of planktic foraminifer shells. By contrast, the current dataset is the first to compare GSMS $\delta^{18}O$ values from roasted and unroasted material from isotopically identical foraminifer shell fragments.

The effect of organic contamination on SIMS $\delta^{18}O$ values is difficult to evaluate with the data at hand and, unfortunately, the effect of roasting on SIMS $\delta^{18}O$ values remains unknown as *in situ* measurements were not performed on unroasted and roasted fragments of the same chambers. Oxygen composes a minor portion of amino acids and

proteins that are present within the foraminifer calcite at low concentrations (King Jr and Hare, 1972; Robbins and Brew, 1990), but the relative sensitivity factors and instrument bias are not known for the conditions of our SIMS analyses. Nevertheless, the consistent $\Delta^{18}O_{SIMS-GSMS}$ values for all experiments (Fig. 4) suggest that measurement of refractory organics in the foraminifer calcite by SIMS – and not GSMS – may be a contributing factor to the inter-instrument difference.

4.3.4. SIMS measurement of matrix-bound sulfate

Another secondary, oxygen-bearing phase that may be measured by SIMS but not GSMS is carbonate-associated sulfate (CAS). In *O. universa* calcite, CAS concentration ranges from 1000 to 1800 ppm and tracks the $[SO_4^{2-}]/[Ca^{2+}]$ ratio of seawater (Paris et al., 2014). In order to evaluate whether CAS contributes to the observed $\Delta^{18}O_{SIMS-GSMS}$, we reference analysis of a calcite speleothem, where CAS concentrations are known to track atmospheric SO_2 sourced by volcanogenic and anthropogenic emissions (e.g. Frisia et al., 2008; Wynn et al., 2010; Borsato et al., 2015). Consequently, CAS concentrations in speleothem calcite have increased by a factor of 10 (from < 10 ppm to ~100 ppm) during the past ~150 years due to fossil fuel emissions (Frisia et al., 2008; Wynn et al., 2010; Borsato et al., 2015). Yet, $\Delta^{18}O_{SIMS-GSMS}$ values measured in a speleothem that grew continuously from pre-industrial to modern are temporally invariant within SIMS analytical precision (± 0.5‰, 2SD; Orland, 2012). The observation that speleothem $\Delta^{18}O_{SIMS-GSMS}$ values do not measurably scale with CAS concentration suggests that low amounts of CAS (10–100 ppm) do not contribute to the $\delta^{18}O$ offset. However, SIMS analysis of the relatively high CAS concentration (~1000 ppm) in foraminifers is still a possible explanation for the $\Delta^{18}O_{SIMS-GSMS}$ values reported herein for *O. universa* calcite.

4.3.5. SIMS measurement of matrix-bound water

Biogenic carbonates contain water within the organic or carbonate matrix, on grain boundaries, in fluid inclusions, and/or chemically bound to the matrix as OH^- ions (Gaffey, 1988). Thus, another contribution to the SIMS-GSMS $\delta^{18}O$ difference may be from other contaminants in the foraminifer matrix, such as water or hydroxyl ions. An important result of this study is that the roasted chambers ($n = 13$) have lower OH/O ratios than the untreated, cleaned, and cultured chambers, but still have a comparable SIMS-GSMS $\delta^{18}O$ offset (Fig. 7). SIMS analyses on basaltic glass at the University of Wisconsin-Madison indicate that 1 wt% water increases OH/O ratios by approximately 0.002. The relative sensitivity factors for glass and carbonate will differ, but this comparison provides an approximate value for the weight percent of water. Assuming the relative sensitivity factors are equal, the untreated, cleaned, and cultured shells (~0.011) have water contents that are consistent with those (~3 wt%) previously reported for skeletal carbonates (Hudson, 1967; Gaffey, 1988, 1990). The removal of unbonded water in the foraminifer shell, rather than removal of OH or organics or a change in shell matrix, during roasting is the most likely explanation for the lower OH/O ratios of our roasted shell fragments (Fig. 7). Results from a prior study show that samples roasted *in vacuo* at temperatures (150 °C for 8 h and 105 °C for 24 h) lower than those used in this study have a reduced H_2O and OH absorption signal in the reflected 0.5–2.5 μm wavelength spectra (Gaffey et al., 1991). The comparable $\Delta^{18}O_{SIMS-GSMS}$ values registered by the untreated, cleaned, and roasted chambers suggest that the H-bearing phase, most likely unbonded water, lost during roasting is not a major factor in the SIMS-GSMS $\delta^{18}O$ difference. Although unroasted foraminifers are exposed to high vacuum prior to and during SIMS analysis, we cannot rule out SIMS measurement of chemically bound water in foraminifer calcite.

4.3.6. Measurement of secondary calcite phases

Field studies have shown that many mixed-layer dwelling species sink into deeper, cooler waters during reproduction (gametogenesis) at the end of their life cycles where an ^{18}O–enriched crust is rapidly added to the outer surface of a shell (e.g. Bé, 1980; Duplessy et al., 1981;

Lohmann, 1995; Kozdon et al., 2009). Approximately 4 μg of gameto-genic (GAM) calcite is added to the outer surface of *O. universa* shells during the final 24 h of calcification (Hamilton et al., 2008) near the deep chlorophyll maximum as the species transitions from its normal life through meiosis and gamete production (Bé, 1980). In addition, diagenesis can add sub-micrometer to micrometer scale carbonate phases onto foraminifer shells at relatively cold bottom-water tem-peratures, which would then bias whole-shell GSMS measurements of planktic foraminifers toward higher-δ^{18}O values (Killingley, 1983; Pearson et al., 2001, 2007; Sexton et al., 2006; Kozdon et al., 2013; Edgar et al., 2015). Unfortunately, measuring the δ^{18}O of such minute (< 3 μm) early diagenetic crystallites (e.g. Groeneveld et al., 2008) and thin GAM crusts (~2 μm) on *O. universa* with SIMS is precluded by their proximity to the epoxy mounting medium. Moreover, the secondary calcite phases cannot be removed or separated prior to GSMS analysis and would, in theory, contribute to the SIMS-GSMS δ^{18}O difference.

The *O. universa* shells recovered from the core-top sample exhibit variable surface structures and optical appearances, which may be at-tributed to diagenetic alteration or the addition of GAM calcite (Fig. S5A-E). However, the $\Delta^{18}O_{SIMS-GSMS}$ values are not dependent upon *O. universa* shell surface textures or optical appearances (Fig. S5F-G), which suggests that the SIMS-GSMS differences are not related to inter-shell differences in preservation or gametogenesis. Moreover, the cul-tured *O. universa* chambers analyzed in this study were never exposed to water column or seafloor conditions, yet they still yield an average $\Delta^{18}O_{SIMS-GSMS}$ value of −0.7 ± 0.1‰. This result suggests that the selective analysis of diagenetic or GAM crust by only GSMS is an un-likely cause of the inter-instrument δ^{18}O difference.

5. Conclusions

Paired δ^{18}O measurements were performed on the final (spherical) chamber of the same *O. universa* shell using *in situ* SIMS and acid-di-gestion GSMS analyses, permitting the direct comparison of the two analytical techniques. Analysis of individual foraminifer chambers was carried out on specimens grown in laboratory culture and fossil (Holocene) shells collected from the upper 3 cm of a sediment core. Comparison of the two datasets yields an average $\Delta^{18}O_{SIMS-GSMS}$ value of −0.9 ± 0.1‰ – an inter-instrumental offset that equates to a ~4 °C difference in reconstructed temperatures (Mulitza et al., 2003). Treat-ment of the core-top shells did not remove the inter-instrument differ-ence given that the $\Delta^{18}O_{SIMS-GSMS}$ values are statistically indis-tinguishable between experiments. Strong positive covariance between the inter-shell SIMS and GSMS δ^{18}O values indicates that secular var-iation expressed in foraminifer δ^{18}O stratigraphies compiled via con-ventional GSMS analyses is captured by SIMS analyses of age-equiva-lent foraminifers.

The inter-instrument δ^{18}O differences measured in this study likely stem from a combination of such factors as SIMS measurement of oxygen in chemically-bound water and refractory organic matter, sample treatment and conditions during GSMS analysis, differences in minor element concentration of samples vs. standards, and/or a change in the SIMS oxygen isotope instrumental mass fractionation due to the differing crystalline microstructures of the foraminifer shells in com-parison to the coarse single crystals of the UWC-3 calcite standard. Determining the roles of these various mechanisms in causing the inter-instrument differences herein reported will require further testing. Furthermore, we caution that the 0–2‰ SIMS-GSMS differences mea-sured for carbonates in this and other studies (Orland et al., 2015) may not exist for δ^{18}O analyses performed on foraminifer taxa with sig-nificantly different shell microstructures, porosities, and/or burial his-tories. This is especially true for foraminifer shells recovered from older, more deeply buried sediments that have experienced a greater degree of degradation of organic compounds (Gaffey, 1990) and release water bound within the shell matrix (Gaffey, 1985). Thus, this study motivates future research to investigate the causes of these differences.

References

Adelseck Jr., C.G., 1978. Dissolution of deep-sea carbonate: preliminary calibration of preservational and morphologic aspects. Deep-Sea Res. II 25, 1167–1185.

Allison, N., Finch, A.A., EIMF, 2010. The potential origins and palaeoenvironmental implications of high temporal resolution δ^{18}O heterogeneity in coral skeletons. Geochim. Cosmochim. Acta 74, 5537–5548.

Bé, A.W., 1980. Gametogenic calcification in a spinose planktonic foraminifer, *Globigerinoides sacculifer* (Brady). Mar. Micropaleontol. 5, 283–310.

Bé, A.W., Harrison, S., Lott, L., 1973. *Orbulina universa* d'Orbigny in the Indian Ocean. Micropaleontology 19, 150–192.

Bemis, B.E., Spero, H.J., Bijma, J., Lea, D.W., 1998. Reevaluation of the oxygen isotopic composition of planktonic foraminifera: experimental results and revised paleo-temperature equations. Paleoceanography 13, 150–160.

Bender, M.L., Lorens, R.B., Williams, D.F., 1975. Sodium, magnesium and strontium in the tests of planktonic foraminifera. Micropaleontology 21, 448–459.

Berger, W.H., 1968. Planktonic foraminifera: selective solution and paleoclimatic inter-pretation. Deep-Sea Res. II 15, 31–43.

Berger, W.H., 1970. Planktonic foraminifera: selective solution and the Lysocline. Mar. Geol. 8, 111–138.

Borsato, A., Frisia, S., Wynn, P.M., Fairchild, I.J., Miorandi, R., 2015. Sulphate con-centration in cave dripwater and speleothems: long-term trends and overview of its significance as proxy for environmental processes and climate changes. Quat. Sci. Rev. 127, 1–13.

Boyle, E.A., 1981. Cadmium, zinc, copper, and barium in foraminifera tests. Earth Planet. Sc. Lett. 53, 11–35.

Carpenter, S., Lohmann, K.C., 1992. Sr/Mg ratios of modern marine calcite: empirical indicators of ocean chemistry and precipitation rate. Geochim. Cosmochim. Acta 56, 1837–1849.

Coplen, T.B., Kendall, C., Hopple, J., 1983. Comparison of stable isotope reference samples. Nature 302, 236–238.

Cuif, J.P., Dauphin, Y., Nehrke, G., Nouet, J., Perez-Huerta, A., 2012. Layered growth and crystallization in calcareous biominerals: impact of structural and chemical evidence on two major concepts in invertebrate biomineralization studies. Fortschr. Mineral. 2, 11–39.

Delaney, M.L., Bé, A.W., Boyle, E.A., 1985. Li, Sr, Mg, and Na in foraminiferal calcite shells from laboratory culture, sediment traps, and sediment cores. Geochim. Cosmochim. Acta 49, 1327–1341.

Duplessy, J.C., Blanc, P.L., Bé, A.W., 1981. Oxygen-18 enrichment of planktonic for-aminifera due to gametogenic calcification below the euphotic zone. Science 213, 1247–1250.

Edgar, K.M., Anagnostou, E., Pearson, P.N., Foster, G.L., 2015. Assessing the impact of diagenesis on δ^{11}B, δ^{13}C, δ^{18}O, Sr/Ca and B/Ca values in fossil planktic foraminiferal calcite. Geochim. Cosmochim. Acta 166, 189–209.

Eggins, S., Sadekov, A., DeDeckker, P., 2004. Modulation and daily banding of Mg/Ca in tests by symbiont photosynthesis and respiration: a complication for seawater ther-mometry? Earth Planet. Sc. Lett. 225, 411–419.

Eiler, J.M., Valley, J.W., Graham, C.M., 1997. Standardization of SIMS Analysis of O and C isotope ratios in Carbonates from ALH-84001. Lunar Planet. Sci. XXVIII Lunar Planet. Inst., Houston. #327(abstr.).

Eiler, J.M., Valley, J.W., Graham, C.M., Fournelle, J.H., 2002. Two populations of car-bonate in ALH84001: geochemical evidence for discrimination and genesis. Geochim. Cosmochim. Acta 66, 1285–1303.

Emiliani, C., 1966. Paleotemperature analysis of Caribbean cores P6304-8 and P6304-9

and a generalized temperature curve for the past 425,000 years. Geology 74, 109–124.

Epstein, S., Buchsbaum, R., Lowenstam, H.A., Urey, H.C., 1953. Revised carbonate-water isotopic temperature scale. Bull. Geol. Soc. Am. 64, 1315–1326.

Erez, J., Honjo, S., 1981. Comparison of isotopic composition of planktonic foraminifer in plankton tows, sediment traps, and sediments. Palaeogeogr. Palaeoclimatol. 33, 129–156.

Fehrenbacher, J.S., Spero, H.J., Russell, A.D., Vetter, L., Eggins, S., 2015. Optimizing LA-ICP-MS analytical procedures for elemental depth profiling of foraminifera shells. Chem. Geol. 407-408, 2–9.

Frankowiak, K., Wang, X.T., Sigman, D.M., Gothmann, A.M., Kitahara, M.V., Mazur, M., Meibom, A., Stolarski, J., 2016. Photosymbiosis and the expansion of shallow-water corals. Sci. Adv. 2, 1–7.

Frisia, S., Borsato, A., Susini, J., 2008. Synchrotron radiation applications to past volcanism archived in speleothems: an overview. J. Volcanol. Geotherm. Res. 177, 96–100.

Gaffey, S., 1985. Reflectance spectroscopy in the visible and near-infrared (0.35-2.55 μm): applications in carbonate petrology. Geology 13, 270–273.

Gaffey, S.J., 1988. Water in skeletal carbonates. J. Sediment. Petrol. 58, 397–414.

Gaffey, S., 1990. Skeletal versus nonbiogenic carbonates UV-visible-near IR (0.3–2.7 μm) reflectance properties. In: Coyne, L.M., McKeever, S.W., Blake, E.S. (Eds.), Spectroscopic Characterization of Minerals and Their Surfaces. 415. Am. Chem. Soc., Washington, D.C., pp. 94–116.

Gaffey, S., Kolak, J., Bronnimann, C.E., 1991. Effects of drying, heating, annealing, and roasting on carbonate skeletal material, with geochemical and diagenetic implications. Geochim. Cosmochim. Acta 55, 1627–1640.

Groeneveld, J., Nurnberg, D., Tiedemann, R., Reichart, G.J., Steph, S., Reuning, L., Crudeli, D., Mason, P., 2008. Foraminiferal Mg/Ca increase in the Caribbean during the Pliocene: Western Atlantic warm pool formation, salinity influence, or diagenetic overprint? Geochem. Geophys. Geosyst. 9, 1–21.

Hamilton, C.P., Spero, H.J., Bijma, J., Lea, D.W., 2008. Geochemical investigation of gametogenic calcite addition in the planktonic foraminifera *Orbulina universa*. Mar. Micropaleontol. 68, 256–267.

Hanson, N.N., Wurster, C.M., Todd, C.D., EIMF, 2010. Comparison of secondary ion mass spectrometry and micromilling/continuous flow isotope ratio mass spectrometry techniques used to acquire intra-otolith $\delta^{18}O$ values of wild Atlantic salmon (Salmo salar). Rapid Commun. Mass Spectrom. 24, 2491–2498.

Hemleben, C., Spindler, M., Anderson, O., 1989. Modern Planktonic Foraminifera. Springer-Verlag, New York.

Hudson, J.D., 1967. The elemental composition of the organic fraction, and the water content, of some recent and fossil mollusc shells. Geochim. Cosmochim. Acta 31, 2361–2378.

Jacob, D.E., Wirth, R., Agbaje, O.B.A., Branson, O., Eggins, S.M., 2017. Planktic foraminifera form their shells via metastable carbonate phases. Nat. Commun. 8, 1–9.

Killingley, J.S., 1983. Effects of diagenetic recrystallization on $^{18}O/^{16}O$ values of deep-sea sediments. Nature 301, 594–597.

Kim, S.T., O'Neil, J.R., 1997. Equilibrium and nonequilibrium oxygen isotope effects in synthetic carbonates. Geochim. Cosmochim. Acta 61, 3461–3475.

King Jr., K., Hare, P.E., 1972. Amino acid composition of planktonic foraminifera: a paleobiochemical approach to evolution. Science 175, 1461–1463.

Kita, N.T., Ushikubo, T., Fu, B., Valley, J.W., 2009. High precision SIMS oxygen isotope analysis and the effect of sample topography. Chem. Geol. 264, 43–57.

Kolodny, Y., Bar-Matthews, M., Ayalon, A., McKeegan, K.D., 2003. A high spatial resolution $\delta^{18}O$ profile of a speleothem using an ion-microprobe. Chem. Geol. 197, 21–28.

Kozdon, R., Ushikubo, T., Kita, N.T., Spicuzza, M.J., Valley, J.W., 2009. Intratest oxygen isotope variability in the planktonic foraminifer *N. pachyderma*: real vs. apparent vital effects by ion microprobe. Chem. Geol. 258, 327–337.

Kozdon, R., Kelly, D.C., Kita, N.T., Fournelle, J.H., Valley, J.W., 2011. Planktonic foraminiferal oxygen isotope analysis by ion microprobe technique suggests warm tropical sea surface temperatures during the Early Paleogene. Paleoceanography 26, 1–17.

Kozdon, R., Kelly, D.C., Kitajima, K., Strickland, A., Fournelle, J.H., Valley, J.W., 2013. *In situ* $\delta^{18}O$ and Mg/Ca analyses of diagenetic and planktic foraminiferal calcite preserved in a deep-sea record of the Paleocene-Eocene thermal maximum. Paleoceanography 28, 517–528.

Lea, D.W., Boyle, E.A., 1991. Barium in planktonic foraminifera. Geochim. Cosmochim. Acta 55, 3321–3331.

Lea, D.W., Mashiotta, T.A., Spero, H.J., 1999. Controls on magnesium and strontium uptake in planktonic foraminifera determined by live culturing. Geochim. Cosmochim. Acta 63, 2369–2379.

Linzmeier, B.J., Kozdon, R., Peters, S.E., Valley, J.W., 2016. Oxygen isotope variability within nautilus shell growth bands. PLoS One 11, 1–31.

Liu, Y., GuoQiang, T., XiaoXiao, L., ChaoYong, H., XianHua, L., 2015. Speleothem annual layers revealed by seasonal SIMS $\delta^{18}O$ measurements. Sci. China Earth Sci. 58, 1741–1747.

Lohmann, G.P., 1995. A model for variation in the chemistry of planktonic foraminifera due to secondary calcification and selective dissolution. Paleoceanography 10, 445–457.

McCrea, J.M., 1950. On the isotopic chemistry of carbonates and a paleotemperature scale. J. Chem. Phys. 18, 849.

Mulitza, S., Boltovskoy, D., Donner, B., Meggers, H., Paul, A., Wefer, G., 2003. Temperature: $\delta^{18}O$ relationships of planktonic foraminifera collected from surface waters. Palaeogeogr. Palaeoclimatol. 202, 143–152.

de Nooijer, L.J., Spero, H.J., Erez, J., Bijma, J., Reichart, G.J., 2014. Biomineralization in perforate foraminifera. Earth Sci. Rev. 135, 48–58.

Oehlerich, M., Baumer, M., Lücke, A., Mayr, C., 2013. Effects of organic matter on carbonate stable isotope ratios ($\delta^{13}C$, $\delta^{18}O$ values) - implications for analyses of bulk sediments. Rapid Commun. Mass Spectrom. 27, 707–712.

Orland, I., 2012. Seasonality from speleothems: High-resolution ion microprobe studies at Soreq Cave, Israel. In: Ph.D. Thesis. University of Wisconsin-Madison.

Orland, I.J., Bar-Matthews, M., Kita, N.T., Ayalon, A., Matthews, A., Valley, J.W., 2009. Climate deterioration in the Eastern Mediterranean as revealed by ion microprobe analysis of a speleothem that grew from 2.2 to 0.9 ka in Soreq Cave, Israel. Quat. Res. 71, 27–35.

Orland, I., Kozdon, R., Linzmeier, B.J., Wycech, J., Sliwiński, M.G., Kitajima, K., Kita, N.T., Valley, J.W., 2015. Enhancing the Accuracy of Carbonate $\delta^{18}O$ and $\delta^{13}C$ Measurements by SIMS. American Geophysics Union Conference, San Francisco #PP52B-03(abstr.).

Paris, G., Fehrenbacher, J.S., Sessions, A.L., Spero, H.J., Adkins, J.F., 2014. Experimental determination of carbonate-associated sulfate $\delta^{34}S$ in planktonic foraminifera shells. Geochem. Geophys. Geosyst. 15, 1452–1461.

Pearson, P.N., 2012. Oxygen isotopes in foraminifera: overview and historical review. Paleontol. Soc. Pap. 18, 1–38.

Pearson, P.N., Ditcheld, P.W., Singano, J., Harcourt-Brown, K.G., Nicholas, C.J., Shackleton, N.J., Hall, M.A., 2001. Warm tropical sea surface temperatures in the Late Cretaceous and Eocene epochs. Nature 415, 481–487.

Pearson, P.N., Van Dongen, B.E., Nicholas, C.J., Pancost, R.D., Schouten, S., Singano, J.M., Wade, B.S., 2007. Stable warm tropical climate through the Eocene Epoch. Geology 35, 211–214.

Potts, P.J., 1992. Gas source mass spectrometry. In: A Handbook of Silicate Rock Analysis Springer US, pp. 546–565.

Ren, H., Sigman, D.M., Meckler, A.N., Plessen, B., Robinson, R.S., Rosenthal, Y., Haug, G.H., 2009. Foraminiferal isotope evidence of reduced nitrogen fixation in the ice age Atlantic Ocean. Science 323, 244–248.

Robbins, L.L., Brew, K., 1990. Proteins from the organic matrix of core-top and fossil planktonic foraminifera. Geochim. Cosmochim. Acta 54, 2285–2292.

Rollion-Bard, C., Mangin, D., Champenois, M., 2007. Development and application of oxygen and carbon isotopic measurements of biogenic carbonate by ion microprobe. Geostand. Geoanal. Res. 31, 39–50.

Russell, A.D., Honisch, B., Spero, H.J., Lea, D.W., 2004. Effects of seawater carbonate ion concentration and temperature on shell U, Mg, and Sr in cultured planktonic foraminifera. Geochim. Cosmochim. Acta 68, 4347–4361.

Sadekov, A.Y., Eggins, S.M., De Deckker, P., 2005. Characterization of Mg/Ca distributions in planktonic foraminifera species by electron microprobe mapping. Geochem. Geophys. Geosyst. 6, 1–14.

Schrag, D.P., DePaolo, D.J., Richter, F.M., 1995. Reconstructing past sea surface temperatures: correcting for diagenesis of bulk marine carbonate. Geochim. Cosmochim. Acta 59, 2265–2278.

Sexton, P.F., Wilson, P.A., Pearson, P.N., 2006. Microstructural and geochemical perspectives on planktic foraminiferal preservation: "Glassy" versus "Frosty". Geochem. Geophys. Geosyst. 7, 1–29.

Śliwiński, M.G., Kitajima, K., Kozdon, R., Spicuzza, M.J., Fournelle, J.H., Denny, A., Valley, J.W., 2016. Secondary ion mass spectrometry bias on isotope ratios in dolomite-ankerite, part I: $\delta^{18}O$ matrix effects. Geostand. Geoanal. Res. 40, 157–172.

Śliwiński, M., Kitajima, K., Spicuzza, M.J., Orland, I.J., Ishida, A., Fournelle, J.H., Valley, J., 2017. SIMS bias on isotope ratios in Ca-Mg-Fe carbonates (part III): $\delta^{18}O$ and $\delta^{13}C$ matrix effects along the magnesite-siderite solid-solution series. Geostand. Geoanal. Res. 42, 49–76.

Spero, H., 1988. Ultrastructural examination of chamber morphogenesis and biomineralization in the planktonic foraminifer *Orbulina universa*. Mar. Biol. 99, 9–20.

Spero, H., Lea, D.W., 1993. Intraspecific stable isotope variability in the planktic foraminifera *Globigerinoides sacculifer*: results from laboratory experiments. Mar. Micropaleontol. 22, 221–234.

Spero, H., Parker, S.L., 1985. Photosynthesis in the symbiotic planktonic foraminifer *Orbulina universa*, and its potential contribution to oceanic primary productivity. J. Foraminifer. Res. 15, 273–281.

Spero, H., Bijma, J., Lea, D.W., Bemis, B.E., 1997. Effect of seawater carbonate concentration on foraminiferal carbon and oxygen isotopes. Nature 390, 497–500.

Spero, H.J., Eggins, S.M., Russell, A.D., Vetter, L., Kilburn, M.R., Honisch, B., 2015. Timing and mechanism for intratest Mg/Ca variability in a living planktic foraminifer. Earth Planet. Sci. Lett. 409, 32–42.

Treble, P.C., Schmitt, A.K., Edwards, R.L., McKeegan, K.D., Harrison, T.M., Grove, M., Cheng, H., Wang, Y.J., 2007. High resolution secondary ionisation mass spectrometry (SIMS) $\delta^{18}O$ analyses of Hulu Cave speleothem at the time of Heinrich event 1. Chem. Geol. 238, 197–212.

Valley, J.W., Kita, N.T., 2009. *In situ* oxygen isotope geochemistry by ion microprobe. In: Fayek, M. (Ed.), In MAC Short Course: Secondary Ion Mass Spectrometry in the Earth Sciences. vol. 41. pp. 16–63.

Vetter, L., Kozdon, R., Mora, C.I., Eggins, S.M., Valley, J.W., Honisch, B., Spero, H.J., 2013. Micron-scale intrashell oxygen isotope variation in cultured planktic foraminifers. Geochim. Cosmochim. Acta 107, 267–278.

Vihtakari, M., Renaud, P.E., Clarke, L.J., Whitehouse, M.J., Hop, H., Carroll, M.L., Ambrose Jr., W.G., 2016. Decoding the oxygen isotope signal for seasonal growth patterns in Arctic bivalves. Palaeogeogr. Palaeoclimatol. 446, 263–283.

Wacker, U., Fiebig, J., Schoene, B.R., 2013. Clumped isotope analysis of carbonates:

comparison of two different acid digestion techniques. Rapid Commun. Mass Spectrom. 27, 1631–1642.

Weidel, B.C., Ushikubo, T., Carpenter, S.R., Kita, N.T., Cole, J.J., Kitchell, J.F., Pace, M.L., Valley, J.W., 2007. Diary of a bluegill (Lepomis macrochirus): daily $\delta^{13}C$ and $\delta^{18}O$ records in otoliths by ion microprobe. Can. J. Fish. Aquat. Sci. 64, 1641–1645.

Wright, I.P., 1998. Gas source mass spectrometry. In: Encyclopedia of Earth Science.

Springer, Netherlands, pp. 261–262.

Wycech, J., Kelly, D.C., Marcott, S., 2016. Effects of seafloor diagenesis on planktic for-aminiferal radiocarbon ages. Geology 44, 551–554.

Wynn, P.M., Fairchild, I.J., Frisia, S., Spötl, C., Baker, A., Borsato, A., EIMF, 2010. High-resolution sulphur isotope analysis of speleothem carbonate by secondary ionisation mass spectrometry. Chem. Geol. 271, 101–107.